

SECTION 9

RISK ASSESSMENT

	Page
RELIABILITY ANALYSIS METHODS FOR SEDIMENT PROBLEMS --	
Ben Chie Yen and Charles S. Melching.....	9-1
FLUVIAL SEDIMENT MEASUREMENTS IN SW SAUDI ARABIA --	
Harold P. Guy and Gavin S. Hamilton.....	9-9
UNCERTAINTY IN ESTIMATES OF SUSPENDED SEDIMENT LOAD --	
Ed Gilroy.....	9-17

RELIABILITY ANALYSIS METHODS FOR SEDIMENT PROBLEMS

By Ben Chie Yen, University of Virginia, Charlottesville; and Charles S. Melching, Rutgers, The State University of New Jersey, Piscataway.

ABSTRACT

Considerable progress has been made recently on reliability analysis in engineering. Some of the newly developed techniques are applicable to sediment problems including transport, erosion, measurements, and gaging networks. In this paper these techniques and their potential applicabilities are briefly introduced. Particularly, application to quantitative risk determination for dam safety and bridge pier scour are discussed.

INTRODUCTION

Estimation of sediment detachment, transport, and deposition is highly uncertain due to the dependence of these processes on the three-dimensional structure of turbulent flow and the stochastic nature of the size and shape of the sediment. Such estimates are further complicated due to uncertain knowledge of flow boundaries in movable bed channels and of design discharges and their corresponding hydraulic conditions, e.g., flow unsteadiness and nonuniformity (Yen, 1988). Reliability analysis could systematically account for these uncertainties and greatly aid engineering practice in sedimentation by providing a flexible, unbiased, and consistent way to consider the combined effect of the various sources of uncertainty on sediment problems.

Reliability concepts and methods are not unknown in sedimentation engineering. For example, Kron and Plate (1988) presented the initial development of the joint probability distribution function of the bed elevation and the design scour (corresponding to the design discharge) for an example of a quay wall along a constricted section of the channel. Also de Groot et al. (1988) presented a new design method for bed protection wherein the depth of bed protection is selected such that the probability that scour will remove the entire protective layer during the life of the structure is below some acceptable level. The probability distribution of scour was determined from combination of the uncertainty in the transport equation, the bed shear stress frequency distribution, and the transformation of transport to scour.

A purpose of this paper is to further stimulate the interest in and application of reliability analysis in sedimentation engineering by presenting some of the existing reliability analysis techniques and illustrating how reliability analysis may aid in bridge scour design and earth dam safety evaluation.

METHODS FOR COMPONENT RELIABILITY ANALYSIS

For individual components of a complex engineering system or for a simple engineering system the reliability, R_L , may be expressed as the probability that the resistance (or capacity), R , of the system exceeds the load, L , placed on it:

$$R_L = \Pr (R \geq L) \quad (1)$$

placed on it:

$$R_L = \Pr (R \geq L) \quad (1)$$

Both the load and resistance are, generally, functions of other basic variables whose probability distributions or statistical properties may be reasonably estimated. For example, the scour "load" on a bridge pier is a function of the discharge, the models used to convert discharge to hydraulic conditions and to determine scour, and the parameters of these models. The purpose of reliability analysis methods is to aggregate the probability information (uncertainties) of the basic variables into the probability distribution of a function which describes the system's performance:

$$R_L = \Pr (Z \geq 0) \quad (2)$$

where Z = system performance function which may be taken as the marginal safety $R - L$, or safety factor in the form of $\ln (R/L)$, or occasionally $(R/L)-1$, depending on the reliability analysis method chosen and the probability characteristics of the basic variables.

A number of methods have been proposed by various investigators for the calculation of the reliability of single component engineering systems, including (but not limited to) the methods of: return period, direct integration, Monte Carlo simulation, reliability index, mean-value and advanced first-order second-moment (MFOSM and AFOSM, respectively) analysis. A qualitative comparison of these methods is given in Table 1. The method of

Table 1. General comparison of reliability calculation methods
(after Yen, 1986)

Method	Return Period	Direct Integration	Monte Carlo	Reliability Index	MFOSM	AFOSM
Capability to account for different factors	very limited	limited	yes	yes	yes	yes
Information needed on probability distribution of factors	indirectly	extensive	moderate	first two statistical moments	only the combined distribution, for factors the first two statistical moments suffice	only the combined distribution, for factors the first two statistical moments suffice
Complexity in application	simple	complicated	moderately complicated	moderate	moderate	moderate
Amount of computations	simple	moderate to extensive	extensive	moderate to simple	moderate to simple	moderate
Capability to estimate total risk	no	difficult	extensive computations	no	yes	yes
Result adaptable for risk cost analysis	partial	yes	yes	no	yes	yes

return period is the current "state of practice" and it is an incomplete reliability indicator, the uncertainties in the hydraulic and sediment transport models and in the bed material are ignored. Kron and Plate (1988) used direct integration to show that for an allowable erosion depth of 11.67 m (design resistance) if the real resistance varies uniformly between 11 m and 12 m the failure probability of a quay wall designed for the 100-year discharge is actually 1/75. This illustrates the need for more complete reliability consideration using the other methods. Details of these reliability analysis methods are presented in Yen and Tung (1991) and Yen (1986). References in Yen (1986) further illustrate the application of these reliability analysis methods in the design of hydraulic structures such as culverts, levees, storm sewers, and dam overtopping.

FAULT TREE ANALYSIS AND RELIABILITY PROCEDURE

A fault tree is a diagram showing the adverse conditions (faults) and their interrelations which could potentially lead to failure of a complex system. Faults may include technical failure of the system elements, extremal geophysical events, operational and management faults, and aggressive human actions. It allows division of work to different people in different disciplines for evaluating the system reliability. Figure 1 illustrates the basic components of a fault tree. A teamwork approach between disciplines coordinated by the fault tree would be likely in most applications of reliability analysis in sedimentation engineering. For example, bridge pier undermining due to scour is only a small part of the overall fault tree for estimation of the reliability of a bridge design.

The construction of a fault tree begins with the identification of a main failure event (top event) whose probability of occurrence is to be estimated. The fault tree is then a graphical decomposition of the top event into the union and/or intersection of subevents that could lead to the top event. The decomposition is continued until a primary or secondary failure event is reached. Primary events are basic inherent failures of a system element whose probability may be assessed via the reliability analysis methods discussed previously. Secondary events are purposely not developed further due to lack of information or of sufficient models to further describe this event (e.g., human error). Switch events represent events whose occurrence will change the operating condition of the system. The OR gate (union of events) indicates that the occurrence of any one of the branches will result in a failure. The AND gate (intersection of events) indicates a failure will occur if all the branch events under the gate occur simultaneously.

Application of fault tree analysis in hydraulic engineering has not been extensive, and, yet, impressive successes have been obtained. For example, fault tree analysis was used in the design of the more than \$1 billion Eastern Scheldt storm surge barrier in The Netherlands (Vrijling, 1982).

EXAMPLE OF BRIDGE SCOUR

The current practice in foundation design for bridge piers to protect against undermining as specified by the American Association of State Highway and Transportation Officials (1989, p. 51) is

"Stream piers and arch abutments shall be founded at a

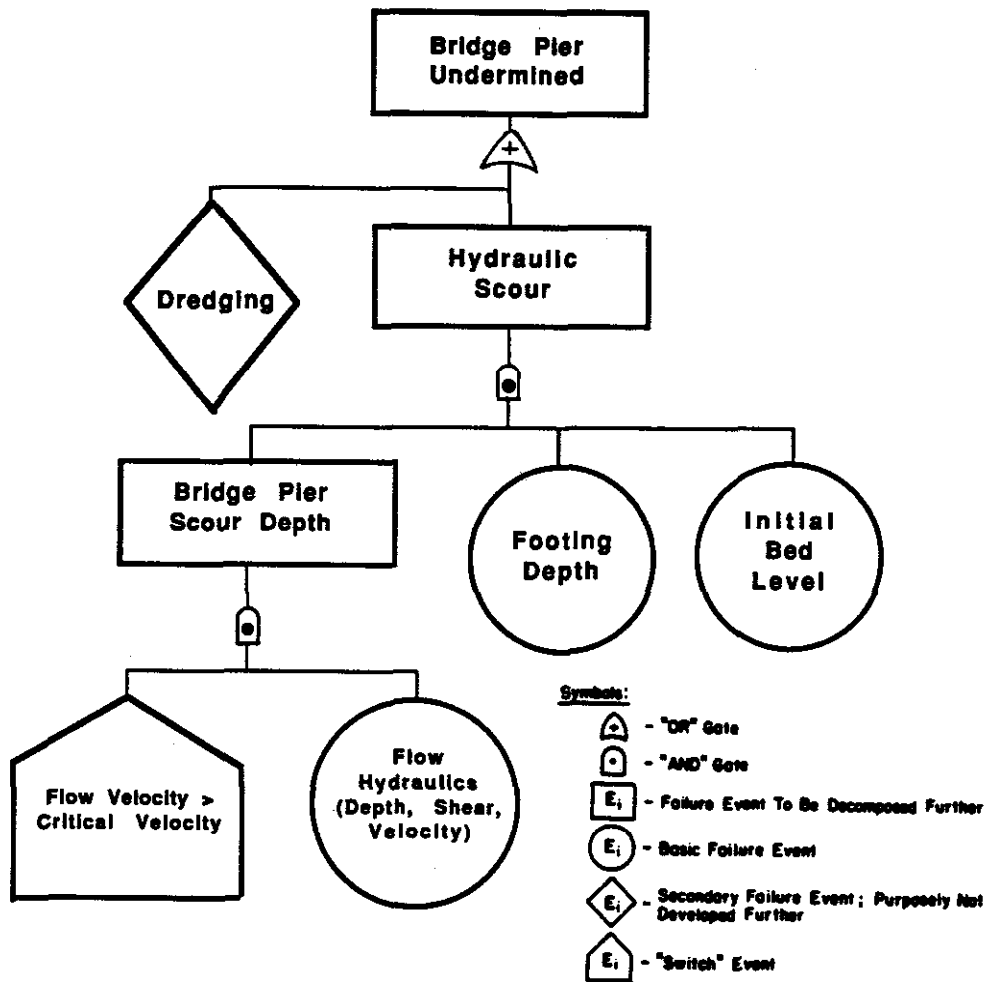


Figure 1. Fault tree for estimating the probability of bridge pier undermining.

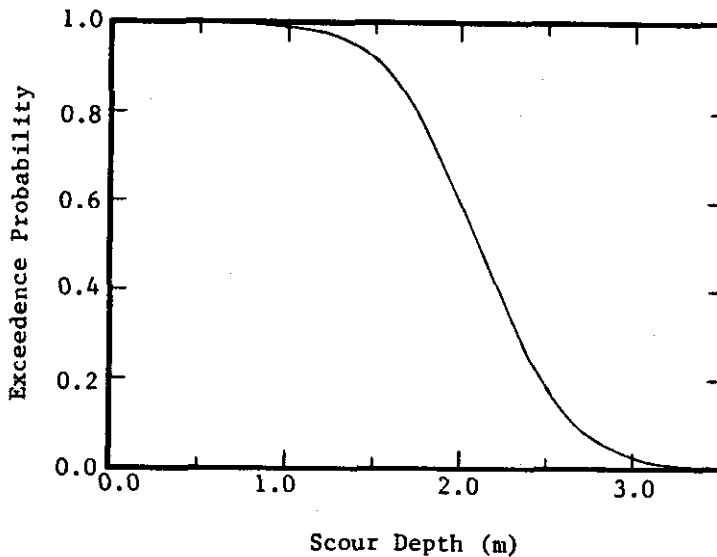


Figure 2. Bridge pier scour exceedence probability.

depth preferably not less than 6 feet below stream bed.
The above preferred minimum depths shall be increased
as conditions may require."

The phrase "as conditions may require" is evaluated by selection of an appropriate method for estimation of local scour. Because of the difficulty of evaluating the flow pattern and the shear forces generated by the flow pattern around a bridge pier, most of the data upon which estimates of depth of scour are made have been obtained by experiments (Vanoni, 1975, p.63). Numerous equations exist for depth of scour estimation, most are based on experiments for cylindrical piers with adjustment factors accounting for different pier shapes, flow angle of attack, and bridge pier spacing. Melville and Sutherland (1988) propose an envelope curve method for estimating bridge pier scour for design. The envelope curve provides an upper bound for scour based on much of the existing laboratory data for cylindrical piers under both live bed and clear water scour conditions.

Given that envelope curves and minimum foundation depths are the dominant criteria for design of bridge piers free from undermining, the introduction of reliability analysis has great potential to improve design practice by defining the tradeoff between cost and reliability. The Hydraulic scour branch of Figure 1 shows the fault tree for estimating the probability of bridge pier undermining due to scour. The Flow Hydraulics basic event is determined from the frequency distribution for design floods and the uncertainties in the hydraulic model used to convert the design discharge into the design flow depth, velocity, and boundary shear. The switch event of "Flow Velocity > Critical Velocity" reflects the change in scour as the system switches from clear water to live bed conditions. The Initial Bed Level basic event is the frequency distribution of the bed level which may be approximated via time series simulation of flow and transformation into bed levels (including consideration of hydraulic and sediment transport model uncertainties) as suggested by Kron and Plate (1988).

To illustrate the estimation of the probability distribution for bridge pier scour depth consider a simple hypothetical example of a 100m wide rectangular channel with a slope = 0.005, Manning's $n = 0.03$ and carrying a discharge of $320 \text{ m}^3/\text{s}$. The coefficient of variation of these four variables are, respectively in the above mentioned order, 0.05, 0.1, 0.2 and 0.202. The design discharges are lognormally distributed and Manning's equation describes flow hydraulics. Finally, assume that Neill's (1964) approximation to Laursen and Toch's (1956) scour design curves is adequate to estimate scour for this case of cylindrical piers. Neill's equation is of the form

$$d_s = A B^{0.7} y_o^{0.3} \quad (3)$$

where d_s = depth of scour, B = bridge pier width, y_o = upstream flow depth, A = empirical coefficient equal to 1.5. To account for the uncertainties in this scour model it is assumed that A is actually a random variable with a mean of 1.5 and a coefficient of variation of 0.2.

Figure 2 displays the exceedence probability as a function of scour depth as estimated by the AFOSM method. The scour depth for the 100-year discharge

(500 m³/s) using the mean hydraulic and scour parameters is 2.29 m. From Fig. 2 it can be seen that this conventional design depth has a 33 percent chance of being exceeded while a scour depth of 3.15 m would be required if a 1 percent failure probability were acceptable (assuming all other uncertainties are negligible).

EXAMPLE OF EARTH DAM OVERTOPPING

Earth embankment dams have different failure modes due to different causes. An example fault tree for an earth dam is shown in Fig. 3. An evaluation of the safety of the dam requires the analysis of all the branches of the fault tree which would involve the service of specialists in various disciplines. Cheng (1982) investigated the overtopping risk due to flood and high wind for the Lake-in-the-Hills Dam near Crystal Lake in McHenry County, Illinois. This dam was declared unsafe in the National Dam Safety Inspection Program for being unable to pass 0.5 Probable Maximum Flood on normal reservoir pool level, at top of the spillway crest.

Let H_0 be the initial reservoir water level, h_G denote the height of reservoir water raised by the flood and/or wind, and H_C the height of the dam embankment. The performance variable in Eq. 2 is $Z = H_C - H_0 - h_G$. Referring to the fault tree (Fig. 3) considering only the component of flow overtopping risk, the failure risk P_f can be written as

$$P_f = P(E_1 \cup E_2 \cup E_3) = 1 - P(\bar{E}_1) \cdot P(\bar{E}_2) \cdot P(\bar{E}_3) \quad (4)$$

in which P denotes probability and \bar{E}_i is the nonoccurrence of the event E_i . Let P_F , P_W and P_{FW} be the probability of occurrence induced by flood alone, wind alone, and wind and flood, respectively. Assuming the occurrences of flood and wind are statistically independent, each following a Poisson process, the flow overtopping risk over a time period T is

$$P_f(T) = 1 - \exp[-T(\nu_F P_F + \nu_W P_W + \nu_{FW} P_{FW})] \quad (5)$$

in which ν is the mean occurrence rate in years which can be estimated based on past statistical data or from other reasoning. The values of P_F , P_W , and P_{FW} are determined by using the AFOSM method considering the randomness of the following variables: rainfall depth, duration, and frequency; hyetograph shape; soil and its antecedent moisture; initial reservoir stage; watershed size; length of main flow path and slope; spillway length, height, breadth, and discharge coefficient; wind speed, direction, and frequency; fetch; and reservoir depth along fetch.

The computed flow overtopping risk is shown in Fig. 4. This risk is only a component of the total dam failure risk. It should be combined with other components of the fault tree in Fig. 3 to yield the total dam failure risk.

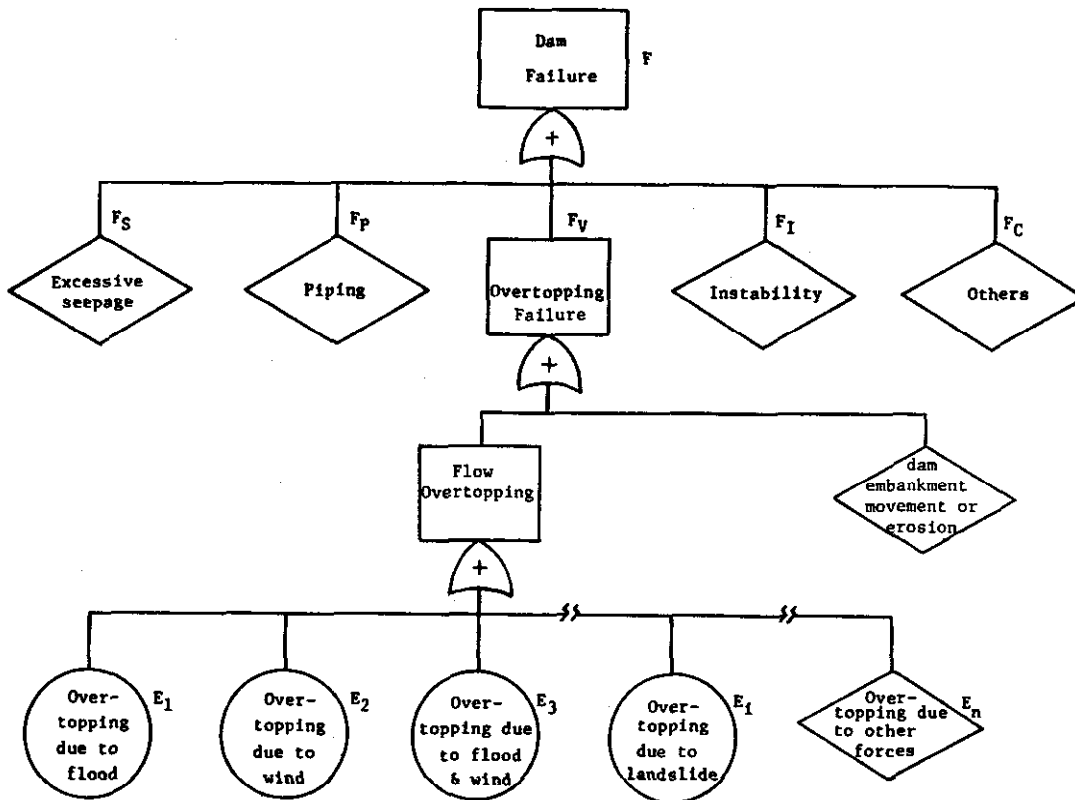


Figure 3. Simple fault tree for an existing dam.

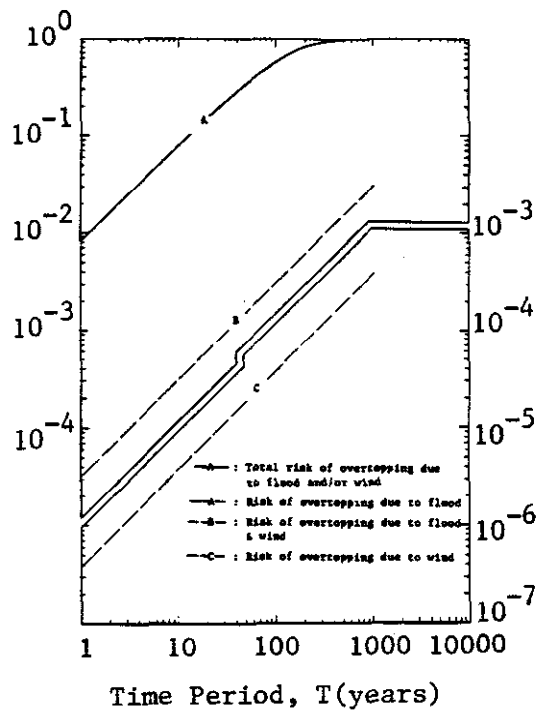


Figure 4. Comparison of overtopping risks induced by different geophysical forces (after Cheng, 1982).

CONCLUDING REMARKS

Existing reliability analysis techniques can be applied to many sediment problems, such as land erosion risk, levee and embankment safety, silting of reservoirs, lakes and ponds, settling basin efficiency, sediment transport and channel resistance model reliability, gaging network planning and design, determination of sampling accuracy and frequency, just to name a few. Some techniques may be more suitable than others for some specific problems. However, in many cases the MFOSM or AFOSM analysis appears to be most practical, allowing consideration of many variables without requiring a large amount of data nor the probability distributions of the variables.

In this paper applications of reliability analysis techniques to bridge scour and earth dam flow overtopping risk are presented as examples. Specific application of reliability analysis to sediment problems is still relatively new. Much still needs to be done for applications to different kinds of problems.

REFERENCES

- American Association of State Highway and Transportation Officials, 1989, Standard Specifications for Highway Bridges, Fourteenth Edition. Washington, DC.
- Cheng, S.-T., 1982, Overtopping Risk Evaluation for an Existing Dam. Ph.D. Thesis, Dept. of Civil Engrg., Univ. of Illinois at Urbana-Champaign, Urbana, Illinois.
- de Groot, M.B., Bliet, A.J., and van Russum, H., 1988, Critical Scour: New Bed Protection Design Method. J.Hyd. Engrg., ASCE. 114 (10), 1227-1240.
- Kron, W., and Plate, E.J., 1988, Reliability of Hydraulic Structures in Rivers with Unstable Beds - Problems of Instationary Sediment Transport. Proc. Fifth IAHR Int. Symp. on Stochastic Hydraulics, Birmingham, U.K.
- Laursen, E.M., and Toch, A., 1956, Scour Around Bridge Piers and Abutments. Bulletin No. 4, Iowa Highway Research Bd.
- Melville, B.W., and Sutherland, A.J., 1988, Design Method for Local Scour at Bridge Piers. J. Hyd. Engrg., ASCE 114 (10), 1210-1226.
- Neill, C.R., 1964, River-bed Scour, A Review for Engineers. Canadian Good Roads Assn., Tech. Publ. No. 23.
- Vanoni, V.A., ed., 1975, Sedimentation Engineering. ASCE - Manuals and Reports on Engineering Practice - No. 64, New York, pp. 745.
- Vrijling, J.K., 1982, Design of Concrete Structures - Probability Design Method. Proc. Delta Barrier Symposium, Rotterdam, The Netherlands, 44-49.
- Yen, B.C., 1986, Reliability of Hydraulic Structures Possessing Random Loading and Resistance. in Engineering Reliability and Risk in Water Resources, Duckstein, L., and Plate, E.J., eds., NATO ASI Series No. 124, Martinus Nijhoff, Dordrecht, The Netherlands, 95-113.
- Yen, B.C., 1988, Significance of Nonuniform, Unsteady and Nonequilibrium Conditions in Fluvial Channels. Proceedings, IAHR Int. Conf. Fluvial Hydraulics, Budapest, Hungary, 112-118.
- Yen, B.C., and Tung, Y.K., 1991. Some Recent Progress in Reliability Analysis. in Reliability and Uncertainties in Hydraulic Design, Yen, B.C. and Tung, Y.K., eds., ASCE.

FLUVIAL SEDIMENT MEASUREMENTS IN SW SAUDI ARABIA

By Harold P. Guy, Engineer-Sediment Specialist, Boiling Springs, PA and Gavin S. Hamilton,
Project Manager, Five-Wadi Study, Saudi Arabian Dames and Moore, Riyadh, Saudi Arabia.

ABSTRACT

Extensive fluvial sediment measurements were made from 1985-1987 in southwestern Saudi Arabia as a part of an overall water balance study from a network of 19 gaging stations in five basins representative of the region. The data at 14 gaging stations were sufficient for long-term extrapolation by correlation through the respective 50-year flow duration curves. The long-term mean annual sediment concentrations in the five basins ranged from 35,500 g/m³ to 71,700 g/m³ (mean = 48,100 g/m³). The mean annual sediment yields in these basins ranged from 197 t/km² to 1097 t/km² (mean = 351 t/km²). Erosion rates varied from 0.02 mm/year to 0.41 mm/year. At most stations nearly all the sediment discharge occurred in less than one percent of the period of record.

INTRODUCTION

Fluvial sediment measurements in southwestern Saudi Arabia were conducted in five representative basins of the region. The sediment measurement program was a part of an overall study of the water balance in these basins, including surface and ground water flows, surface and ground water quality, evaporation rates, soil moisture movement, and other climatic parameters.

The objective of the sediment studies was to evaluate the magnitude and character of sediment transported by wadis in order to provide data for accommodating, or avoiding, the effects of the sediment on water control facilities and their utilization. The method of evaluation involved the collection of representative samples of the wadi flow for determination of sediment quantity and particle size over a wide range of flows, and extrapolation of these data to wadi flow at other times and to other locations.

Sediment measurements were made at 19 gaging stations within the five basins from late 1984 through 1987. Periodic and storm-event samples were obtained of the flow using standard sediment measurement techniques as described in the U.S. Geol. Survey, "National Handbook for Recommended Methods of Water Data Acquisition", 1977, and Guy and Norman, 1970. Suspended-sediment samples were obtained with a DH-48 (depth-integrating hand-held) sampler. Sediment samples were analyzed in Saudi Arabian Dames & Moore laboratory in Riyadh to determine suspended-sediment concentration and particle size distribution by methods described in the above mentioned "National Handbook", and in Guy, 1969.

Sampling of storm flows was generally limited to periodic observations, but for some flood events, sampling was sufficient to graph the sediment concentration with the flow stage through the hydrograph. The total flow and sediment discharged for the storm event was then computed as the cumulative sum of the incremented measurements during the event (Porterfield, 1972). All observations of suspended-sediment concentration were tabulated for computation of instantaneous suspended-sediment discharge. Both the storm-event and instantaneous sediment discharge data were then available for correlation with water discharge and other parameters.

The particle size of the bed material at each gaging station was obtained in a site survey by a combination of the lesser known stone-count and the well known sieving method (Kelleralls, and Bray, 1971) (Wolman, 1954). By necessity, this combination was used for most gaging stations because of the abundance of gravel, cobble, and sometimes boulder sized particles in the bed of the wadi. A sample of bed material particles included the hand measurement of the intermediate size of one particle at each of more than 200 randomly selected points at each gage. The selected points were defined by either the whole or half-meter locations along a tape stretched across the wadi at two or more sections at or near the gaging station. At points where particle size was generally less than 16 mm, a representative sample of sand was collected for sieving at the laboratory.

DESCRIPTION OF DRAINAGE BASINS

Statistics concerning the gaging-sediment stations of the representative basins are listed in table 1. The hydrological and sediment regimes of the overall study region is affected by the presence of the Asir Escarpment which rises 2,000 to 3,000 meters above sea level. The ridge line runs generally parallel to and about 100 km east of the Red Sea coast.

Wadis Habanah and Tabalah are located east of the ridgeline and flow toward the interior of the Arabian Peninsula. Gradients of the wadis in the eastern basins are generally less steep than those in the western basins.

The study region receives considerably more rainfall than other regions in Saudi Arabia. The source of the rainfall is moisture laden air masses from the Indian Ocean, moving across the Gulf of Aden and the Red Sea. The dominant mechanism for the precipitation is convection, although there is an orographic effect at the escarpment. Predominately, the precipitation regime is of sparse, highly intense, short duration events with extreme spatial variability. Precipitation can occur at all times of the year, but most occurs during spring and fall. Average annual rainfall in the higher elevations approaches 600 mm.

Table 1. Gaging-Sediment Station Statistics.

Number	Station name	Coordinates*		Drainage (km ²)	Elevation (m)**	Bankfull		Channel Slope (m/km)
		Latitude	Longitude			Width (m)	Depth (m)	
LITH BASIN (North Tihama Region)				3079				
J 415	Wadi Lith above Wadi Salibah	204255	403229	949	412.45	60	2	4.54
J 417	Wadi Lith above Wadi Mustanga	203040	402854	1657	208.51	48	2	6.39
J 416	Wadi Dhara near Suq Dahara	204002	402240	274	357.21	110	1.5	9.96
J 418	Wadi Lith near Ghumayqah	202215	402745	2672	114.81	75	1.5	1.72
YIBA BASIN (North Tihama Region)				2830				
SA 422	Wadi Jawf near Tanab	191905	415255	322	550.88	65	2	9.25
SA 401	Wadi Yiba at Suq Thuluth	191655	414845	785	418.53	45	2	4.26
SA 423	Wadi Ghat near Wadi Yiba	190515	414755	597	294.23	180	1.5	5.28
SA 424	Wadi Yiba near Al Hijaya	190045	413800	2305	153.81	110	3	4.20
LIYYAH BASIN (South Tihama Region)				1456				
SA 421	Wadi Khulab at Al Saudie	164440	430540	744	119.15	50	1.5	3.84
SA 425	Wadi Liyyah at Qufi	164130	430500	392	110.12	35	1.5	4.58
SA 426	Wadi Mighyalah near Al Aglah	163810	430430	99	89.53	60	1.5	2.73
HABAWNAH BASIN (Najaran Region)				4930				
N 408	Wadi Sayhan near Al Jifah	174620	435245	1360	1452	70	3	6.58
N 404	Wadi Habawnah near Habawnah	174742	440000	2180	1339	135	2.5	2.24
N 405	Wadi Thar near Thar	175740	440622	940	1303	75	2.5	2.40
N 406	Wadi Habawnah near Lahumah	174938	441658	4320	1212	140	2.5	0.89
SA 407	Wadi Habawnah at Husayniyah	174824	442700	4930	1166	500	2	2.21
TABALAH BASIN (Bishah Region)				1900				
B 413	Wadi Tabalah near Al Alayah	193912	415732	170	1867.63	100	1.5	4.99
B 412	Wadi Tabalah above Wadi Milaha	195552	420637	730	1369.31	100	1.5	4.21
<u>B 405</u>	<u>Wadi Tabalah near Tabalah</u>	<u>200230</u>	<u>421630</u>	<u>1270</u>	<u>1264.92</u>	<u>45</u>	<u>2</u>	<u>4.93</u>
Mean				1405	726	105	2.0	4.48

*The six-number figures are for latitude (north) and longitude (east); two each for degrees, minutes, and seconds.

**Elevation given is that of the gage datum (above mean sea level).

The geology of Wadi Lith Basin is a complex of metavolcanics typically retrograded from amphibolite to green schists facies and granitized by gneissic granite. High mountainous slopes of the Asir Escarpment decrease down to the flat alluvium on the Tihama Plain adjacent to the Red Sea (elevation change is 2,750 m in about 150 km). Eighty-one percent of the basin has very steep slopes (30 to 100 percent). The gentle slope areas are mostly river terraces, outwash, and pedimental deposits.

The Yiba Basin is composed principally of granites (45 percent) and intensely folded Precambrian metamorphosed sedimentary and volcanic rocks. Post Precambrian rocks in the basin are the recent alluvium of the wadi channels, the outwash and pedimental deposits around the batholithic granites. Steep slopes of more than 30 percent occur over more than 50 percent of the basin. Gentle slopes of less than 3 percent occur on less than 10 percent of the basin, mostly as river terraces, outwash and pedimental deposits.

The Liyyah Basin shows a simple west to east geological sequence of granite, chlorite schists, Jurassic quartzitic sandstones, Tertiary volcanics, and Quarternary Tihama sediments. The lower part of the main wadi has wide, but thin sandy and gravelly alluvium. The wadi channel is narrow and sharply incised in the Tertiary volcanic area. Sixty-three percent of the basin has slopes (30-100 percent) and the remainder (0-30 percent). The gentle slope areas are mostly river terraces, outwash and pedimental deposits near the more erodible granites.

The Habawnah Basin geology is predominantly Precambrian granites in the east, schists in the central area, and amphibolite schists and greenstones in the west. The metamorphics of the center and west parts of the basin are more erosion resistant than the granites of the east, therefore the western part of the basin is characterized by a dendritic drainage network of rather narrow gorged channels. Forty-five percent of the basin has very steep slopes (30-100 percent), mostly in the western areas. The gentle slope areas are mostly stream terraces, outwash and pedimental deposits.

The Tabalah Basin is predominantly underlain by granites and grandiorites, with a small area of schistose greenstone in the east, and a zone of amphibolite schists in the center. The rather erodible granites result in low rounded hills with broad flat sandy silty outwash plains between protruding outcrops. The only post precambrian rocks in the basin are the recent alluvium of the wadi channels, and the outwash and pedimental deposits near the batholithic granites. Eighty-one percent of the basin has very steep slopes of 30 to 100 percent and 19 percent has gentle slopes of 0 to 3 percent. The gentle slope areas are mostly wadi terraces.

ANALYSIS OF DATA

Suspended-sediment sample data consisted of 918 observations at 18 gaging stations. See Table 2. Samples taken at J415 were taken at low flows and were not meaningful for analysis. The analysis of sediment data at each gaging station deals with (1) instantaneous observations, (2) storm-event observations, (3) regressions for extrapolating the data in time and space, and (4) sediment adjustment factors. The following briefly describe these analyses.

1. Instantaneous observations: The suspended-sediment concentration data for each sample set was assembled chronologically and multiplied by the wadi flow rate to obtain instantaneous rates of sediment discharge for the times of sampling at each gaging station. As shown in table 2, the number of observations available for this ranged from 0 at station J 415 to 269 at station SA 425. The maximum flow rate sampled was 3,040 m³/s at station SA 423 when the unadjusted suspended-sediment concentration was 91,100 g/m³ and the sediment discharge rate was 276.9 T/s.

2. Storm-event observations: Where the instantaneous data at a station represented several major segments of flow during a 'flood', a sediment concentration graph was plotted on a print of the stage hydrograph and used to compute the sediment discharged for specific intervals throughout the runoff event as described by Porterfield, 1972. The total water (m³) and sediment (T) discharged for the storm event was then compared with that for other storm events. From 4 to 23 storm events were computed in this manner at nine of the nineteen stations. As shown in table 2, station SA 423 had 18 events so computed representing 52 percent of the total runoff and 81 percent of the total sediment for the period of record. Also at station SA 423, the maximum size event was 19,700,000 m³ of flow having an unadjusted sediment discharge of 1,560,000 T during the event.

3. Regressions: Regression equations were developed for both the instantaneous and storm-event sediment data observations. The instantaneous observations were used to develop sediment-water discharge relationships, which in turn were used with the 50-year flow-duration curves of the respective stations to obtain the long-term rate of sediment movement past the gage. The storm-event observations were used to estimate the sediment discharge for unsampled storm events at the respective stations.

4. Sediment adjustment factor: As indicated, the suspended-sediment concentration was sampled with a DH-48 sampler. The limits on ability to wade a wadi during a flood made it necessary to collect many samples from the wadi bank. These bank samples represented the most important segments of the flow for the period of record. Though an attempt was made to select bank sampling points at locations of considerable turbulence, it is logical to assume that such samples were deficient of sediment compared to that carried by the wadi as a whole.

When bank and midstream samples were collected concurrently at the same site, some showed about half the sediment in the bank sample compared with that in the 'midstream' samples, while others were nearly the same. Thus, it can only be concluded that a specifically determined adjustment factor is not possible, especially when there was a need for changing bank sampling locations as the flood stage changed. The sediment adjustment factor for bank samples was arbitrarily set at 1.15. This was applied to the computed results at all stations, including those having many wade-collected samples. The wade-collected samples represent only a very small part of the sediment movement for the period of record.

Table 2. Summary of Suspended-Sediment Sample Data.

Station number	Sediment factor	Instantaneous observations			Storm-event observations				
		Number	Maximum flow rate (m ³ /s)	Maximum sediment disch. (T/s)	Number	Total runoff (%)	Total sediment (%)	Maximum runoff (m ³)	Maximum sediment (T)
J415	1.23	0	-	-	-	-	-	-	-
J417	1.24	54	44.00	1.4818	5	12	12	2,384,000	72,600
J416	1.23	14	205.00	8.8065	1	-	-	863,800	52,300
J418	1.28	112	364.00	114.6236	14	41	49	12,724,600	237,800
SA422	1.23	29	157.00	4.2700	1	-	-	133,900	4230
SA401	1.25	61	362.00	24.4352	4	14	18	2,303,000	130,700
SA423	1.24	75	3,040.00	276.9440	18	52	81	19,700,000	1,560,000
SA424	1.27	17	99.90	5.2448	0	-	-	-	-
SA421	1.30	50	470.00	18.5180	4	8	13	3,720,000	101,000
SA425	1.24	269	554.00	21.5291	23	37	40	6,526,000	211,900
SA426	1.22	58	88.30	0.8318	6	-	-	667,700	5,820
N408	1.22	8	3.80	0.0089	-	-	-	-	-
N404	1.22	20	301.00	20.4680	1	-	-	150,500	3,230
N405	1.24	4	1.92	0.0056	-	-	-	-	-
N406	1.30	47	98.80	12.3698	6	32	36	4,793,000	470,000
N407	1.30	32	24.00	1.7122	3	-	-	2,477,000	230,700
B413	1.26	8	27.49	0.4398	1	-	-	2,750	18
B412	1.24	8	27.80	0.4514	1	-	-	395,200	2,470
B405	1.25	<u>52</u>	87.83	5.0678	<u>12</u>	26	28	1,867,000	39,500
Total		918			100				

When information on total sediment movement is needed, we also must have an adjustment to account for sediment moving below the sampled zone. This is often referred to as bed load movement. Though many studies have been made to measure and estimate the rate of bed load movement relative to measured load, it has generally been concluded (Vanoni, 1975), and the writers concur, that it is not possible to develop a simple rule or formula that will provide a quantitative coefficient for all streams and their various flow conditions. Coefficients of 15 percent for sand-channels and 5 percent for channels having little or no sand is commonly recommended. For the 19 stations in this study, the following was used to compute a coefficient for bed load movement: $\text{Coefficient} = 1.15 - (2/3 \times 0.15 \times \%>4\text{mm}/100)$. For example, at SA 423 where $\%>4\text{mm}$ is 61 (table 4), the coefficient is $1.15 - (2/3 \times 0.15 \times 61/100) = 1.09$.

The bed load and bank sampling coefficients were combined for each station and shown under the heading "Sediment factor" in Table 2. These 'sediment factors' range from 1.22 for rather stoney channels to 1.30 for sand channels.

RESULTS

The suspended-sediment sample data were analyzed as follows to extend information on sediment discharge in time and space:

1. Analyzed sediment discharged for specific storm events, where data were sufficient, by constructing a graph of concentration moving concurrently with the stage hydrograph. The sediment discharge for several time intervals during the storm and the total sediment discharged for the storm event was computed.

2. Used storm-event regression of sediment discharge, tonnes (T) vs. water discharge (m^3/s), to obtain T for unsampled storm events at nine stations. The annual totals for these in terms of T/ km^2 are shown in Table 3.

3. Used all "instantaneous" sample data from both storm-event and periodic sampling to establish a regression equation in terms of sediment discharge (T/s) vs. water discharge (m^3/s) at each station. The grouping of the resulting equation lines is shown in Fig. 1.

4. Used the regression equations of item 3 for 14 stations having 50-year synthetic flow duration curves developed by the project (Saudi Arabian Dames & Moore, 1988) to obtain mean annual sediment discharges at the respective stations.

5. Adjusted the results to account for deficiencies in concentration of samples collected at the bank (+15%) and for material moving below the sampled zone (+5 to 15%), depending on the size of the bed material at the station. The adjusted results are presented in Table 3.

Table 3. Gaging Station Flow and Adjusted Sediment Discharge by Analysis Type.

Storm-event analysis					Flow-duration analysis (50-year)			
<u>Station</u>	<u>Year</u>	<u>Annual flow</u>	<u>Annual sediment</u>	<u>Flow weighted concentration</u>	<u>Station</u>	<u>Annual flow</u>	<u>Annual sediment</u>	<u>Flow weighted concentration</u>
		(m^3/km^2)	(T/ km^2)	(g/ m^3)		(m^3/km^2)	(T/ km^2)	(g/ m^3)
J417	1985	1,920	72	37,200	J417	5,290	335	63,400
J417	1986	5,130	217	42,300	J416	1,640	49	29,900
J417	1987	2,850	61	2130	J418	3,470	207	59,600
J418	1985	1,050	66	64,000	SA422	13,300	427	32,100
J418	1986	5,620	458	81,500	SA401	8,240	468	56,800
J418	1987	3,290	268	81,300	SA423	9,670	268	27,700
SA401	1985	8,830	519	58,700	SA424	4,470	113	25,300
SA401	1986	7,040	388	55,100	SA425	21,470	1,097	51,100
SA401	1987	4,800	51	10,600	N404	8,470	492	58,100
SA423	1985	46,870	3,050	65,100	N406	4,680	304	64,900
SA423	1986	18,770	482	25,700	N407	3,380	311	92,100
SA423	1987	10,790	12	1,110	B413	7,640	117	15,400
SA421	1985	18,700	450	24,000	B412	8,010	458	57,200
SA421	1986	15,460	321	20,800	<u>B405</u>	<u>6,800</u>	<u>274</u>	<u>40,300</u>
SA421	1987	21,780	18	830	Mean	7,609	351	48,136
SA425	1985	57,490	1,978	34,400	Std. dev.	4,819	246	19,830
SA425	1986	52,300	1,152	22,000				
SA425	1987	23,700	418	17,600				
SA426	1985	123,500	2,071	16,800				
SA426	1986	108,600	1,159	10,700				
SA426	1987	57,900	217	3,750				
N406	1985	3,850	367	95,500				
N406	1986	2,200	171	77,000				
N406	1987	0	0	-				
B405	1985	4,830	222	46,000				
B405	1986	2,240	93	41,700				
<u>B405</u>	<u>1987</u>	<u>7,650</u>	<u>132</u>	<u>17,300</u>				
Mean		22,859	534	37,396				
Std. dev.		31,601	726	26,825				

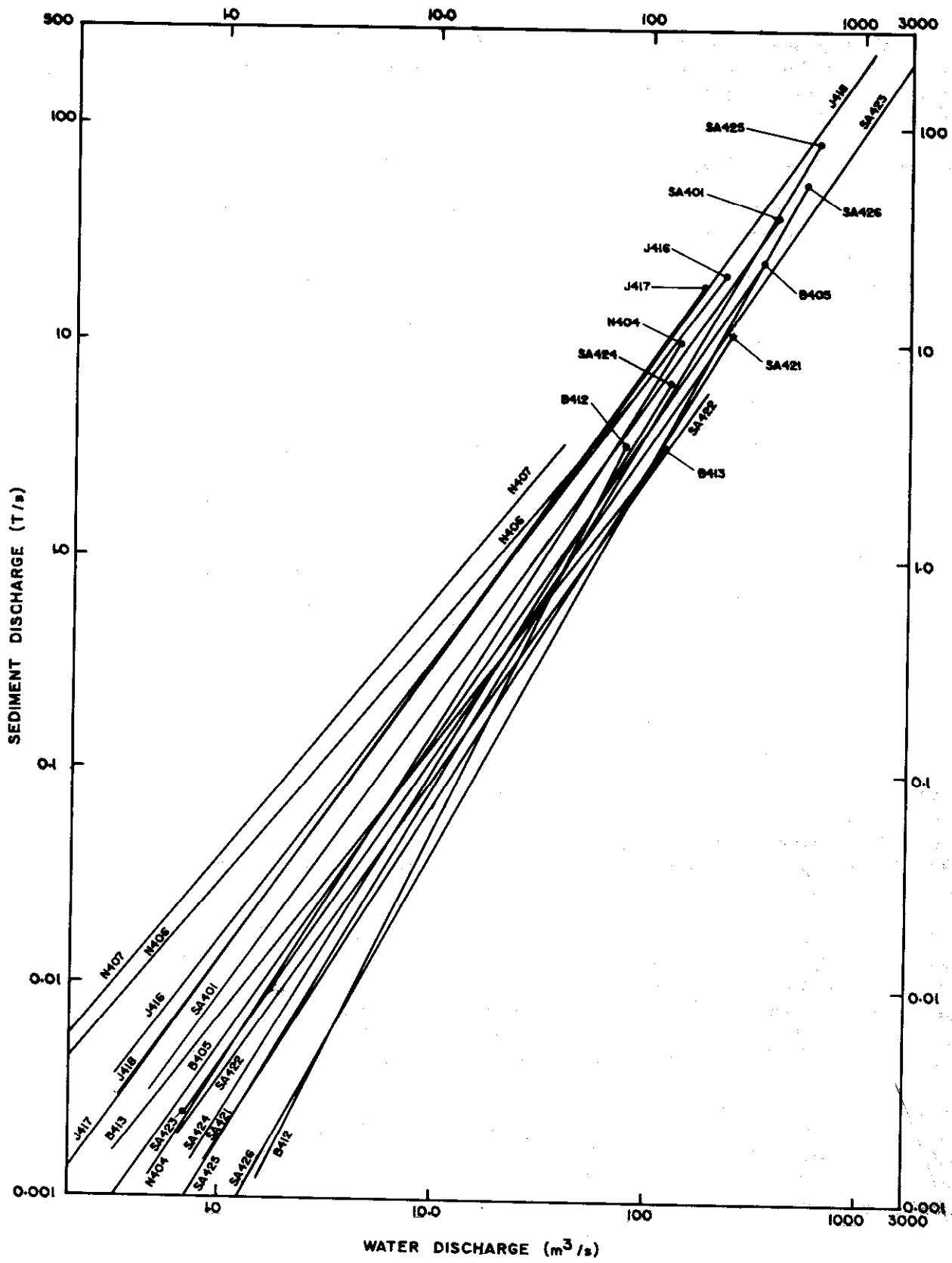


Figure 1. Instantaneous suspended-sediment discharge curves for all stations.

6. Listed particle size information for both suspended sediment and bed material. These are summarized in Table 4 and show that (a) there is no apparent correlation of the suspended-sediment size with the bed material size, (b) bed material size decreased toward sand in the downstream reaches, and (c) there is no apparent difference in suspended sediment sizes among the five basins.

Table 4. Summary of Suspended-Sediment and Bed-Material Particle Data.

Station number	Number of observations*	Suspended sediment			Bed material**		
		Clay %	Silt %	Sand %	D50 (mm)	>4mm %	Ω
J415	-	-	-	-	35	69	79
J417	8	25	57	18	28	61	54
J416	-	-	-	-	31	75	24
J418	13	30	52	18	0.46	20	27
SA422	7	35	50	15	34	71	27
SA401	-	-	-	-	17	52	44
SA423	12	14	57	29	42	61	92
SA424	-	-	-	-	0.57	32	54
SA421	8	36	57	7	0.37	2	3
SA425	21	19	67	14	22	64	28
SA426	-	-	-	-	26	75	17
N408	-	-	-	-	48	79	39
N404	16	29	56	15	27	80	18
N405	-	-	-	-	24	61	56
N406	17	36	52	12	0.32	2	2
N407	13	31	58	11	0.32	2	2
B413	-	-	-	-	2.2	37	9
B412	-	-	-	-	10	59	10
B405	6	<u>31</u>	<u>62</u>	<u>7</u>	<u>5</u>	<u>51</u>	<u>11</u>
Mean		28.6	56.8	14.6	18.6	50.2	31.4
Standard deviation		6.9	4.7	5.8	15.2	25.9	25.3

*Only stations having five or more observations are listed.

**One observation per station consisting of >200 particle measurements at two or more sections near the gage.

Ω A measure of particle size gradation = $1/2(D50/D16 + D84/D50)$.

The notably larger annual sediment concentration and sediment yield at station SA 423 for the storm events record compared to that for the 50-year record is the result of a large flood on April 23, 1985 having an estimated return period of 150 years. During a 25-minute interval of this flood, when the flow rate was 3,210 m³/s and sediment concentration was 111,700 g/m³ (adjusted), 538,200 T of sediment was moved past the gage, or 359 t/s. The total yield for the event was 1,934,000 T in 19,700,000 m³ of flow resulting in a flow weighted mean concentration of sediment of 98,200 g/m³. The effects of this flood on annual sediment yields can be noted also in Table 3 (SA 423, storm events, 1985-87).

As expected from an arid region where the precipitation is usually sparse, highly intense, of short duration, and of extreme spacial variability, the wadi flow occurs in a very small percentage of the time. Because the rate of sediment movement tends to increase in proportion to increasing rates of flow, sediment discharge occurs in a even smaller percentage of the time. This is illustrated in Fig. 2 for Wadi Liyyah (station no. SA 425) where about 92 percent of the sediment and 62 percent of the water is discharged in 0.1 percent of the time.

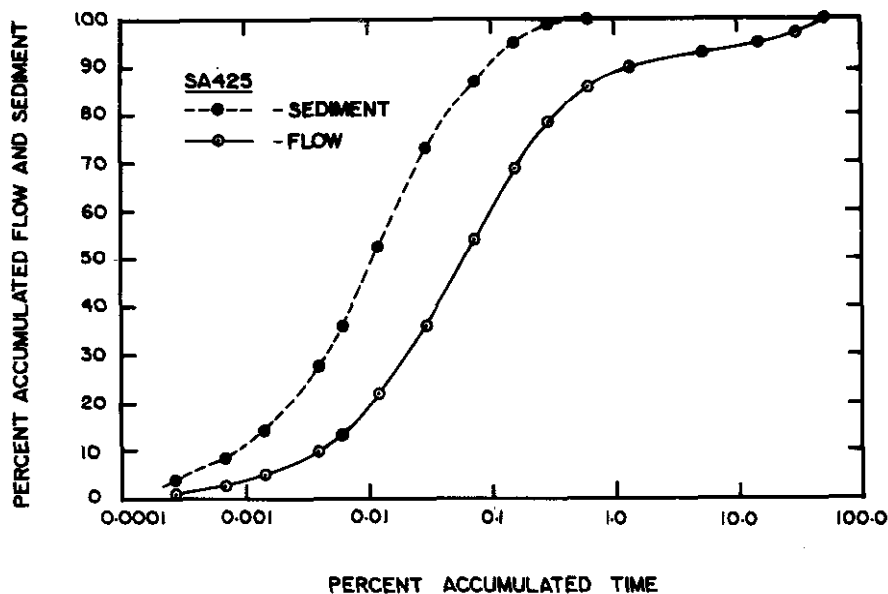


Figure 2. Cumulative flow and sediment discharge; station SA425, Liyyah Basin.

CONCLUSIONS

The geomorphological development of the wadi systems are such that the channels presently contain remnants of previously extensive deposits of sediment. Presently, most transport of this sediment is activated by short intense runoff events, a hydrological characteristic of the region. Fluvial sediment data in the Five Representative Basins show a good degree of homogeneity in the wadi systems. Long term analyses provide a sound basis for extrapolating the results obtained in the Representative Basins to other wadi systems in the south-western region of Saudi Arabia.

ACKNOWLEDGMENTS

The work was carried out for the Water Resources Development Department of the Ministry of Agriculture and Water, Kingdom of Saudi Arabia. The authors wish to thank the Ministry for their support, and, in particular Amer Al Hussein, Director General of the Water Resources Development Department, Misfer Al Kaltham, Chief of Water Research, and Saud Al Tubaishi, Director of the Hydrology Division.

REFERENCES

- Guy, H. P., 1969, Laboratory theory and methods for sediment analysis. U.S. Geol. Survey, Tech. of Water Resources Investigations, Bk. 5, Chap.C1, 58 p.
- Guy, H. P. and Norman, V. W., 1970, Field methods for measurement of fluvial sediment. U.S. Geol. Survey, Tech. of Water Resources Investigations, Bk.3, Chap.C2, 59 p.
- Kellerhals, R. and Bray, D. I., 1971, Sampling procedures for coarse fluvial sediments. J. Hydr. Div., ASCE, 45(8), 1165-1180.
- Miller, C. R., 1951, Analysis of flow-duration sediment-rating curve method of computing sediment yield. U.S. Bur. of Reclamation, Hydraulics Div., 15 p.
- Porterfield, George, 1972, Computation of fluvial-sediment discharge. U.S. Geol. Survey, Tech. of Water Resources Investigations, Bk.3, Chap. C3, 66 p.
- Saudi Arabian Dames & Moore, 1988, Representative basins study for Wadis Yiba, Habawnah, Tabalah, Liyyah, and Lith. Ministry of Agriculture and Water, Kingdom of Saudi Arabia.
- Wolman, M. G., 1954, A method of sampling coarse river-bed material. Am. Geophys. Union Trans., 35(6), 951-956.
- Vanoni, V.A., Editor, 1975, Sedimentation engineering. Amer. Soc. of Civil Engineers, Manuals and Report on Engineering Practices, No 54, p.348.

UNCERTAINTY IN ESTIMATES OF SUSPENDED SEDIMENT LOAD

Ed Gilroy
U. S. Geological Survey
Reston, Virginia

ABSTRACT

The uncertainties of estimates of suspended sediment load are unknown. To approximate a solution to this dilemma, a simple mathematical model is applied to mimic the load-discharge rating curve method used in practice and its associated errors. The uncertainty in sediment loads estimated from this method is given in terms of (1) site-specific measurement errors in the instantaneous concentration measurements, (2) the site-specific parameters of autoregressive-moving average processes used to model the rating curve residuals, (3) the number of concurrent discharge-concentration measurements made each year and (4) a statistical measure of the distance of the distribution of flow data used to calibrate the transport model from the distribution of the flow data used for estimating sediment concentrations.

The uncertainty curves obtained can be used to determine the optimal number of concentration measurements to be made each year or season at a site to achieve a prespecified uncertainty in load estimates, or to determine the uncertainty in sediment loads for a prespecified budget, i.e. a given number of discharge-concentration measurements. Results of these procedures are given for five sites along the Colorado River. The inclusion of higher flows in the sampling scheme is found to be more important in minimizing the uncertainty than is increasing the frequency of sampling beyond a monthly frequency.

Introduction

Estimates of total sediment transported during a given time period are based on measured sediment concentrations and some relation between concentration and water discharge. In the case of a daily-sediment station this relation is based on the experience of a hydrologist familiar with the site of interest who has worked on several years of record at the site. The concentration-discharge curve that exists in the hydrologist's mind is impossible to model exactly by mathematical methods. This makes estimating the uncertainty in estimates of total sediment load for a given time period extremely difficult. As a first step in estimating such uncertainties, the concentration-discharge relation used by the hydrologist is represented by applying a log-linear multiple regression model in which the response variable is the logarithm of concentration (or load) and the explanatory variables are the logarithm of flow, a seasonal term given by the sine and cosine of the day of the year and, an indicator variable denoting whether the flow is on the

rising or falling limb of the hydrograph. The relation is just a transport curve but different from the classical transport curve in which log of flow is the only explanatory variable. Such multiple regression models have been shown (see Thompson et al., 1987) to give estimates of annual sediment loads comparable to estimates obtained by more traditional methods of computing sediment loads for daily stations.

The uncertainty in the estimates of total sediment transport is taken herein as the mean square error of the difference between the estimated total load and the true total load. In order to estimate this mean square error, three steps are necessary. A brief outline of these three steps is given here.

(1) Estimate a sediment rating curve relating instantaneous suspended sediment concentration or load to appropriate explanatory variables. This step is an important one and familiarity with the measurement site is essential to obtain a physically meaningful rating curve.

(2) Compute the set of residuals - measured instantaneous load minus rated instantaneous load - from the rating curve obtained in step (1) and analyze them as a time series. A lag-one autoregressive process is assumed to adequately represent the observed time series of residuals. Three parameters are estimated from the time series - the lag-one-day autocorrelation coefficient, ρ , the process variance, VP and the measurement variance VM . ρ is a measure of the memory in the rating shifts and VP , the process variance, is a measure of the uncertainty in the rating even if there were no measurement error in the instantaneous discharge. This model is virtually the same as that used by Moss and Gilroy (1980).

(3) Use the three parameters obtained in step (2) in a lognormal regression model to obtain the standard error of the estimate of the total transport as a function of the number of suspended sediment measurements made at the site per year.

It is assumed in the lognormal regression model used in the estimation of the uncertainty of sediment loads that the residuals about the multiple linear regression model of the log transformed concentrations are normally distributed and follow a lag-one autoregressive process. Thompson et. al., 1987, show that the lag-one autoregressive process can be used to represent the memory in the residual process of the type of rating curve used here. The normality and autoregressive assumptions allow us to give first estimates of the uncertainty by incorporating some known characteristics of the sediment rating curve method.

Mathematical Model

The relationship between concentration (or equivalently load) and flow is taken to be linear in the logarithms (Gregory and Walling, 1973). The model in this paper considers the same logarithmic structure as in Cohn et. al. (1989) and Gilroy et. al. (1990). Let

$$Y(i) = \ln[L(i)] = \beta_0 + \beta_1 \cdot X_1(i) + \beta_2 \cdot X_2(i) + \dots + \beta_p \cdot X_p(i) + \epsilon(i) \quad (1)$$

for $i = 1, 2, \dots, M$

where $L(i)$ is the i th value of the sediment load, $X_j(i)$ is the i th concurrent value of the j th explanatory variable, the β_j 's are regression coefficients, the $\epsilon(i)$'s are error terms and M is the number of concurrent values of response and explanatory variables.

Let $\hat{Y}(i)$ denote the ordinary least squares estimator of $Y(i)$, the logarithm of load. Because the sediment measurements are commonly taken a month or more apart, the residuals are effectively uncorrelated for the data used to calibrate the log-log regression model. The "rating curve" estimator is simply the exponentiation of $\hat{Y}(i)$, denoted by $\hat{L}(i) = \exp(\hat{Y}(i))$. As is well known - see Cohn et. al. (1989) - this rating curve estimator is biased under the assumption of normally distributed regression residuals. We do not consider the problem of bias in this paper. See Cohn et. al. (1989) and Gilroy et. al. (1990) for more information on the bias correction factor and other properties of various estimators of total load. We consider only the uncorrected rating curve estimator because sediment loads traditionally have been calculated without accounting for the bias correction.

The total load for a time period is given by

$$LTOT = \sum_{i=1}^N L(i).$$

A measured load at time i is denoted by $LM(i)$. The estimate at time i is given by the weighted sum,

$$\tilde{L}(i) = W(i) \cdot \hat{L}(i) + (1-W(i)) \cdot LM(i),$$

which is taken to mimic sediment record computations. The weight $W(i)$ is a function of the uncertainties in both the sediment measurements and the rated values. If no measurement is available at time i then $W(i) = 1$.

The total load for the time period is estimated by

$$LTOT_{HAT} = \sum_{i=1}^N \hat{L}(i)$$

Gilroy et al(1990) give the mean and variance of $\sum_{i=1}^N \hat{L}(i)$, the estimate of LTOT

in the absence of measurements, under the classical assumptions - on the log transformed data - associated with ordinary least squares. Because the assumption is made that the true residuals, $\epsilon(i)$, follow a lag one-day autoregressive process as in Thompson et.al. (1987), the results and methods of Gilroy et al (1990) and Thompson et al (1987) are combined and extended to give the mean square error of the fractional difference

$$DIFF = (LTOT_{HAT} - LTOT) / LTOT.$$

The mean square error of DIFF is a complicated summation of terms involving the parameters obtained in the three steps outlined above and results from manipulation of the moment generating function of a normal distribution. The terms of the summation consist of appropriate forms of the normal moment generating function as in Thompson et al (1987) and Gilroy et al(1990).

RESULTS

Results of these procedures are presented for five sites on the Colorado River.

The results shown are indicative of those to be expected from the application of this type of analysis to the water/sediment discharge sampling questions associated with the Grand Canyon National Park project.

The transport curve model had log of sediment discharge as a linear function of log of water discharge and the sine and cosine of the day of the year as explanatory variables. The results of step (2) - analyzing the time series of residuals - are presented below. These results are based on data for the time period after the Glen Canyon dam was completed.

Table 1. Time series parameters for 5 stations on the Colorado River.

STATION	NUMBER OF MEASUREMENTS	RHO	VP	VM
LEE'S FERRY	233	.72	1.24	.01
L. COL. R.	330	.59	0.86	.01
GRND. CNYN	174	.86	1.19	.01
NAT. CNYN	322	.82	0.97	.01
DMND CRK	298	.86	0.99	.01

The process variance, VP, and measurement variance, VM, are in log base e units so that they are closely related to the variance in percent squared. The standard error of a sediment discharge measurement in percent was taken to be 10 percent based on discussions with experienced hydrologists. Hence VM is .01.

Using these results, uncertainty curves were generated for each of the five stations. Uncertainty curves for two of the stations are given in Figures 1.a-b. The abscissa is in units of distance that the population of calibration flows is from the population of estimation flows. These curves indicate that where one samples in the flow regime is more important than how frequently one samples which agrees with experience.

On the basis of such uncertainty curves, we have some measure of how much uncertainty in estimates of sediment discharge at the five points along the Colorado River, which may help us to rationally determine some sampling strategies. Such curves can be generated for suspended sediment discharge - total suspended, fines and sand separately - and for before and after the dam for the long term sites.

The uncertainty curves will give an estimate of how much reduction in uncertainty is obtained by (1) increased measurement frequency and (2) choosing the calibration flow data to adequately represent the flow regime of interest.

Figure 1.a

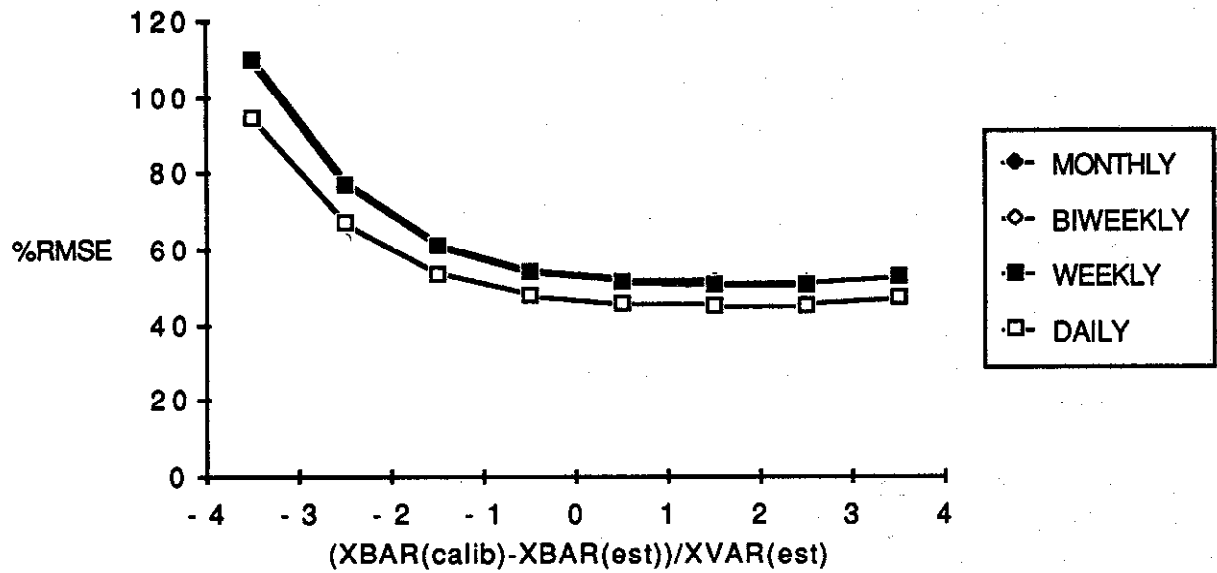


Figure 1.b

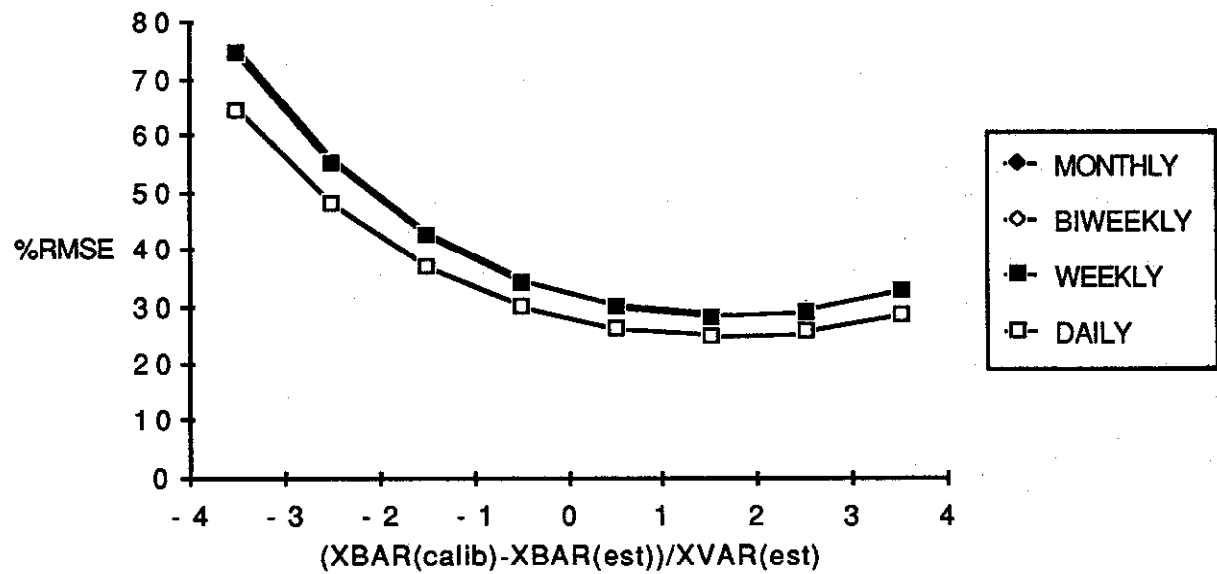


Figure 1. Percent root mean square error of load estimates of suspended fines for a 90-day season as a function of the distance of the mean of the calibration data is from the mean of the estimation data, scaled by the variance of the estimation data. (a) Colorado River at the Little Colorado River and (b) Colorado River at Lee's Ferry. (Monthly to weekly are indistinguishable.)

LIST OF REFERENCES

- Cohn, T. A., L.L. DeLong, E. J. Gilroy, R. M. Hirsch and D. Wells, 1989, Estimating constituent loads, WRR, 25(5), 937-942.
- Gilroy, E. J., R. M. Hirsch, and T. A. Cohn, 1990, Mean square error of regression-based constituent transport estimates , WRR, 26(9), 2069-2077.
- Gregory, K.J. and D.E. Walling , *Drainage Basin Form and Process*, Wiley and Sons, New York, 1973.
- Moss, M. E. and E. J. Gilroy, 1980, Cost-effective stream-gaging strategies for the Lower Colorado River Basin, the Blythe field office operations, USGS Open-file Report 80-1048.
- Thompson, M. E., H. Joe and M. Church, 1987, Statistical modelling of sediment concentration, IWD-HQ-WRB-SS-88-1, Report for the sediment section of Environment Canada.

